Introducing the Inert-Salt in a Solvent-Reduced Catholyte for Improving the Electrochemical Performance

xx, xx and xx[†,]*

[†] xxxxxxxxxxxxxx

*E-mail: xxxxxxxxxx

Supporting Information

Experimental Section

Materials

Lithium metal was received from China Energy Lithium Co. Ltd., 2,2,6,6-tetramethylpiperidine-1-oxyl (TEMPO), lithium hexafluorophosphate (LiPF$_6$), ethylene carbonate (EC) and diethyl carbonate (DEC) were received from Sigma-Aldrich, carbon paper (HCP010N) was received from Shanghai Hesen Electric Co. Ltd., carbon felt (GF020) was received from Suzhou Sinero Technology Co. Ltd., tetrabutylammonium hexafluorophosphate (TBAPF6) was received from Aladdin, silicon (Si) was received from Alfa. The electrolyte of 1 M LiPF$_6$ in EC/DEC (v/v~1:1) was used on the Li metal side in both static and flow mode tests.

Abbreviation of solvent-reduced electrolyte

We abbreviate all the solvent-reduced electrolyte used in this study as *xx* M Li$^+$ + *xx* M TBA$^+$ in T-E (4/1). The '*xx*' represents the concentration of Li$^+$ and TBA$^+$ ions in the solvent-reduced electrolyte. 'T' is the abbreviation for TEMPO and 'E' is the abbreviation for electrolyte with a volume ratio of 4/1. The electrolyte consists of an EC/DEC solvent with a volume ratio of 1:1, which is one of the most commonly used solvent in conventional catholyte.

Preparation of solvent-reduced catholytes

The solvent-reduced catholytes were prepared by utilizing the low-melting-point of TEMPO. Firstly, the TEMPO was heated to melt into a liquid solution at 40 °C. Then a certain amount of LiPF$_6$ salt was added to the above solution and stirred to dissolve, at this time the solution would thereafter solidify after the temperature returned to room temperature. Thirdly, a specific quantity of EC/DEC solvent was incorporated to maintain the solution in a liquid phase at room temperature. To enhance the electrochemical performance of the solution, a certain amount of inert-salt TBAPF$_6$ was further added to complete the preparation of solvent-reduced catholytes.

Assembly of the Li-catholyte static cell

The Li-catholyte hybrid flow battery is a promising high-energy cell configuration which takes advantages of both the high cell voltage of Li-ion battery and scale-up flexibility of RFBs (*J. Am. Chem. Soc.* 2011, 133, 5756-5759). Li-catholyte static cell was used as illustrated in our previous work (H. Chen and Y-C Lu, *Adv. Energy Mater.* **2016**, 1502183). One piece of lithium foil (Φ16 mm) was attached to a bottom cell body. One Celgard 2500 separator (Φ19 mm) was placed on the surface of the lithium foil followed by adding 30 µL of electrolyte (1 M $LiPF_6$ in EC/DEC). One piece of $Li_{1.5}Al_{0.5}Ge_{1.5}(PO_4)_3$ (LAGP) ceramic membrane was placed on the Celgard separator. LAGP can only permit the Li^+ transportation, which ensures charge balance between the Li metal anode and catholyte. The avoiding of the shuttle of active material TEMPO by LAGP improves the cycle stability, rendering it impervious to cross-contamination. The conductivity of LAGP can be preserved during extended cycles (Fig. S11). The highly-concentrated TEMPO-based catholyte encountered severe shuttling effect and rapid capacity decay without LAGP separator as shown in Fig. S12. One piece of carbon paper (Φ12 mm) placed on the LAGP acts as a current collector for catholyte. 20 µL of catholytes were injected to the carbon paper. Finally, a stainless-steel spring and a polytetrafluoroethylene (PTFE) O-ring were placed on the cell. Two cell bodies (bottom and top) were separated by a PTFE spacer to avoid a short circuit. The cell assembling process was conducted in an Ar-filled glove box (Etelux, H_2O < 1.0 ppm O_2 < 1.0 ppm).

Assembly of the Li-catholyte flow cell

Fig. S13 shows the cell configurations of the Li-catholyte flow cell. Carbon felt (Φ12 mm) was used as current collector for the catholytes. Li foil was used as anode and an LAGP lithium-ion ceramic conductor was used as separator to prevent the mixing of anolyte and catholyte and reduce the shuttle effect of TEMPO during charge. A total 5 mL 0.1 M Li^+ + 0.1 M TBA^+ in T-E (4/1) catholytes were used for the continuous flow-mode tests at flow rate of 5 mL min^{-1}. The Masterflex 07528 peristaltic pump (Cole-Parmer, USA) was used to provide the flow pressure.

Electrochemical Characterizations

All the electrochemical characterizations were performed using the Bio-Logic VSP electrochemical workstation. Cyclic voltammogram (CV) tests of catholytes were conducted between 2.9 and 4.1 V vs. Li/Li$^+$ in Li-catholyte static cell configuration with LAGP ceramic separator using carbon paper as the working electrode and the Li metal as reference/counter electrode. Galvanostatic charge-discharge tests were performed between 3.1 and 3.8 V vs. Li/Li$^+$ on using battery testing system (LAND, CT2001A, Wuhan LAND electronics Co., Ltd). Current density was calculated based on the current collector geometric surface area. The volumetric capacity was calculated from the total volume of catholytes. The energy density was calculated by integrating the discharge volumetric capacity and voltage. The *in-situ* UV–vis spectra were collected by SEC2000 UV–visible spectrophotometer (ALS Co., Ltd.) coupled with the VSP electrochemical workstation, at scan rate of 1 mV s^{-1} between the potential ranging from 2.9 to 4.1 V vs. Li/Li$^+$. Electrochemical impedance spectroscopy (EIS) measurements used sinusoidal voltage oscillations of 20 mV amplitude at the open circuit voltage of the cells. The oscillation frequencies were swept from 100 kHz to 100 mHz with three repetitions for every test.

Material Characterizations

The viscosity measurements were conducted using TAINSTRUMENTS AR1000. The samples were dropped into the measurement gap of 0.6 mm on the plate. The contact angle measurements were conducted using OEMDG-01, UK. A 5 μL drop of various catholytes was dropped on a silicon wafer. The contact angle was measured between the droplet and the silicon surface. The differential scanning calorimetry (DSC) analysis was performed on DSC214 NETZSCH. A 10 mg sample was placed in an aluminum pan. The temperature sweep was started by cooling to -150 °C and then heating up to 100 °C with a sweeping rate of 10 °C min^{-1}. The conductivity measurements were conducted on QCF25/100 testing system as shown in

4

Fig. S6. The ionic conductivity measurements were conducted on EUTECH COND6+ as shown in Fig. S7.
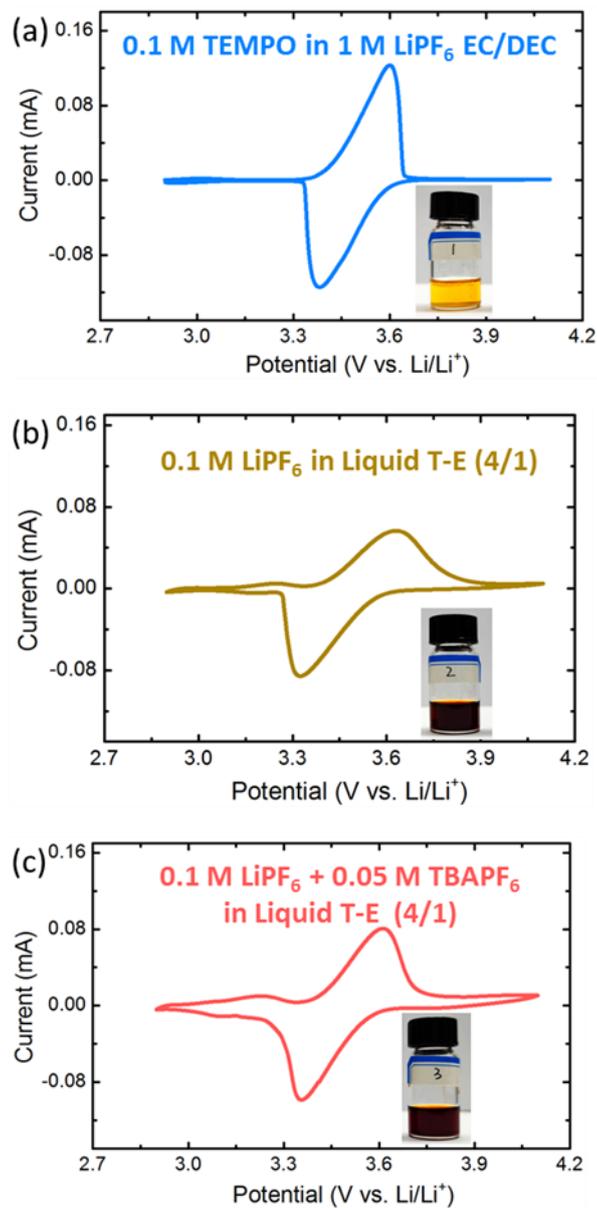
Fig. S1. Cyclic voltammograms (CVs) of (a) 0.1 M TEMPO in 1 M $LiPF_6$ EC/DEC; (b) 0.1 M $LiPF_6$ in T-E (4/1); and (c) 0.1 M $LiPF_6$ + 0.05 M $TBAPF_6$ in T-E (4/1) at 0.1 mV s^{-1}.
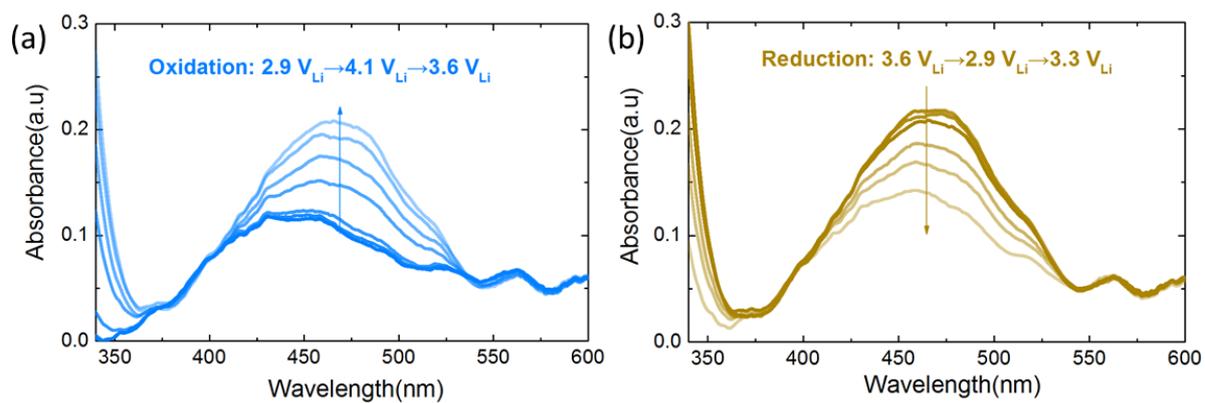
Fig. S2. *In-situ* UV-vis spectra of 0.1 M TEMPO in 1 M LiPF$_6$ EC/DEC (1:1 v/v). (a) Oxidation process and (b) reduction process.
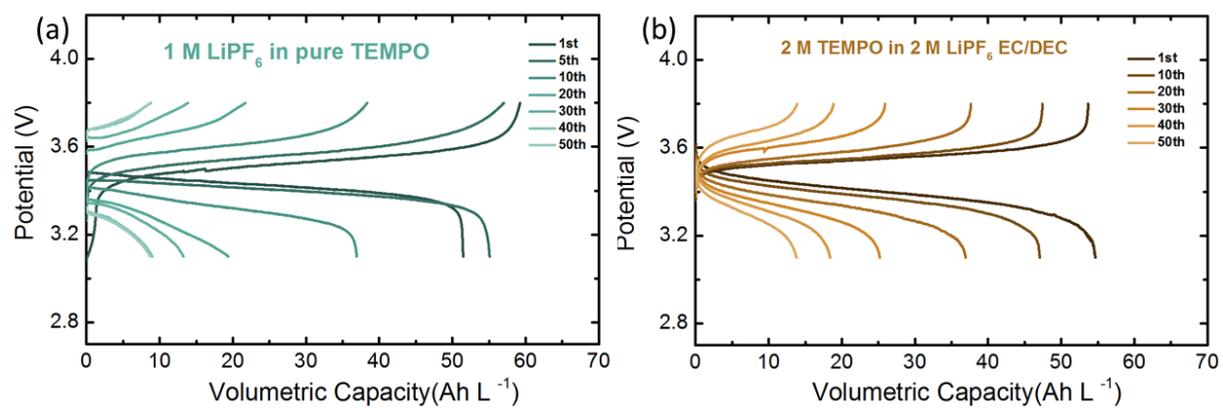
Fig. S3. Galvanostatic charge-discharge profiles of (a) 1 M Li$^+$ in pure melting TEMPO catholyte and (b) 2 M TEMPO in 2 M LiPF$_6$ EC/DEC (1:1 v/v) at 0.1 mA cm^{-2} in Li-catholyte static cell.

Electrolyte	Ionic Conductivity (mS cm^{-1})
1 M Li$^+$ in melting TEMPO	0.292
1 M Li$^+$ in T-E (4/1)	0.671
1 M Li$^+$ + 0.1 M TBA$^+$ in in T-E (4/1)	0.613

Fig. S4. A photograph of ionic conductivity tester and results of different catholytes.
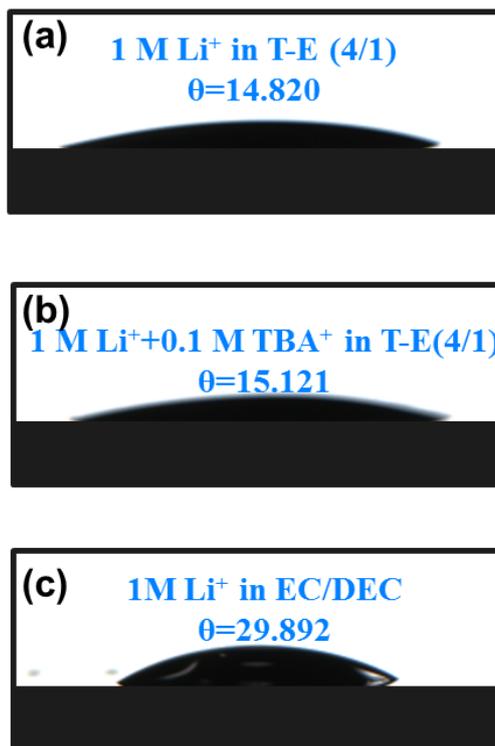
Fig. S5. Contact angel measurement of (a) 1 M Li$^+$ in T-E (4/1); (b) 1 M Li$^+$ + 0.1 M TBA$^+$ in T-E (4/1) and (c) 1 M Li$^+$ in EC/DEC.
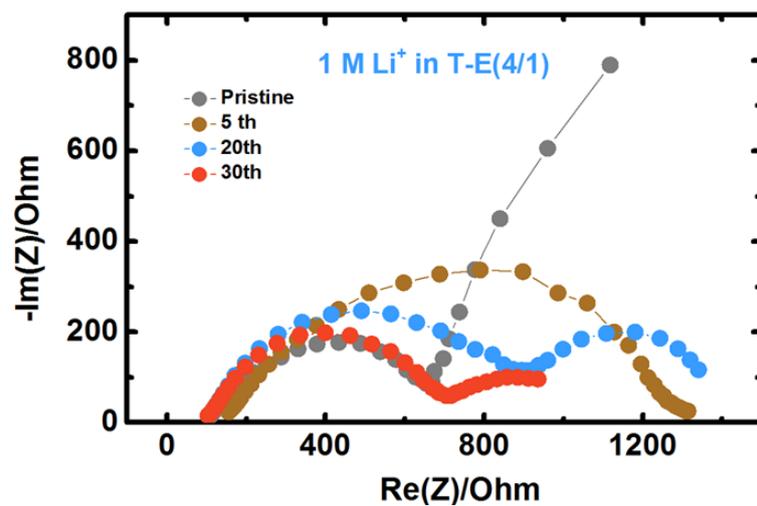
Fig. S6. EIS comparison of 1 M Li$^+$ in T-E (4/1) at various cycling stage.
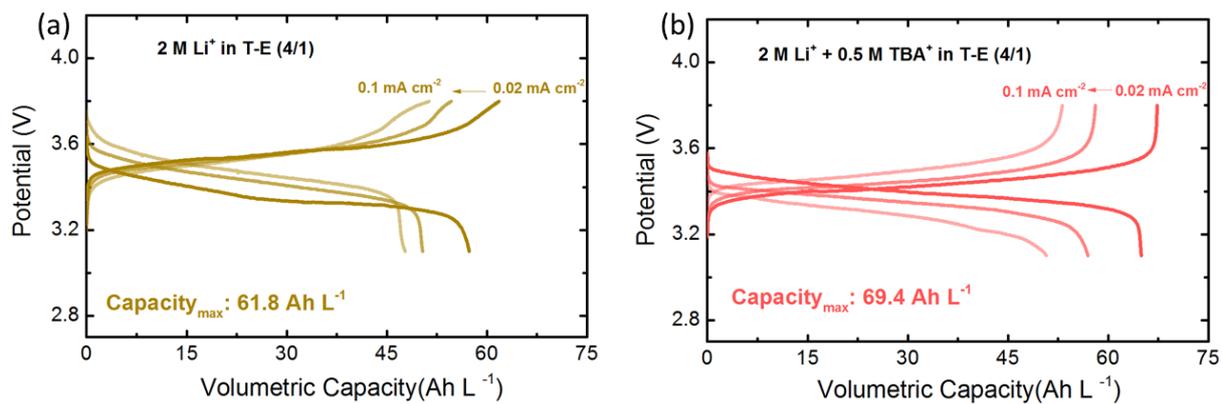
Fig. S7. Galvanostatic charge-discharge profiles of (a) 2 M Li$^+$ and (b) 2 M Li$^+$ + 0.5 M TBA$^+$ in T-E (4/1) at 0.1 mA cm^{-2} in Li-catholyte static cell.
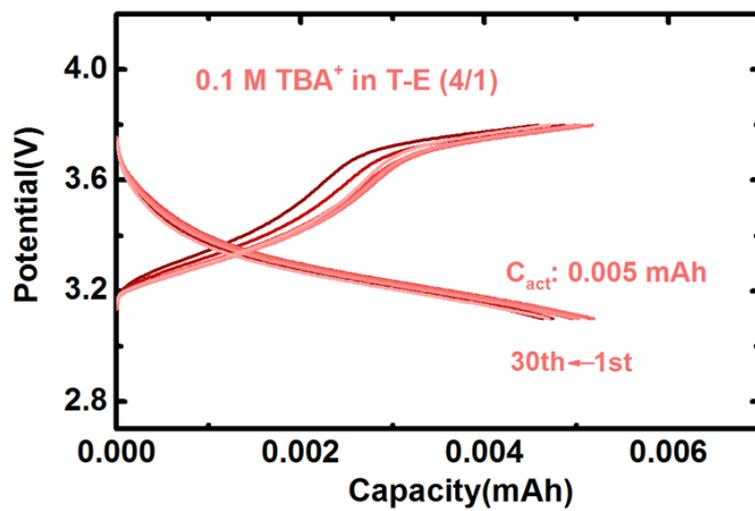
Fig. S8. Galvanostatic charge-discharge profiles of 0.1 M TBA$^+$ in T-E (4/1) at 0.01 mA cm^{-2} in Li-catholyte static cell.
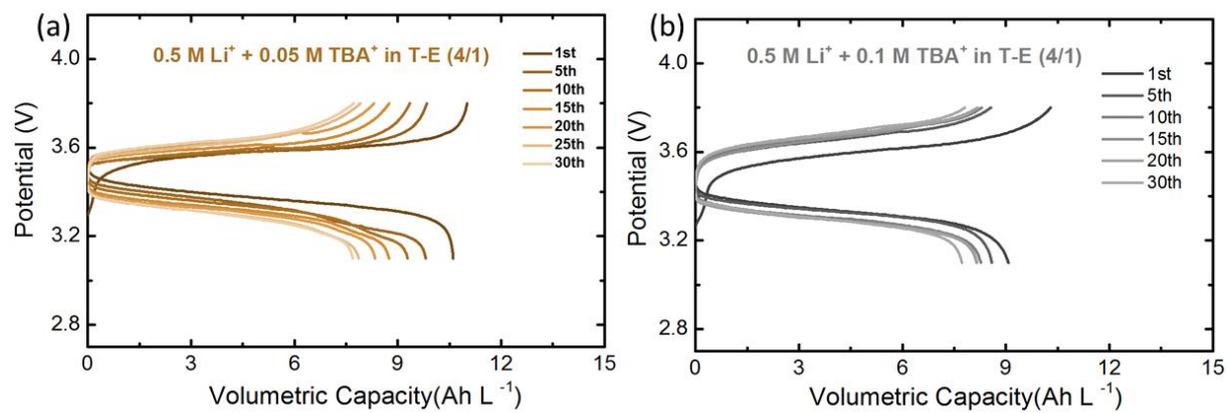
Fig. S9. Galvanostatic charge-discharge profiles of (a) 0.5 M Li^+ + 0.05 M TBA^+ and (b) 0.5 M Li^+ + 0.1 M TBA^+ in T-E (4/1) at 0.1 mA cm^{-2} in Li-catholyte static cell.
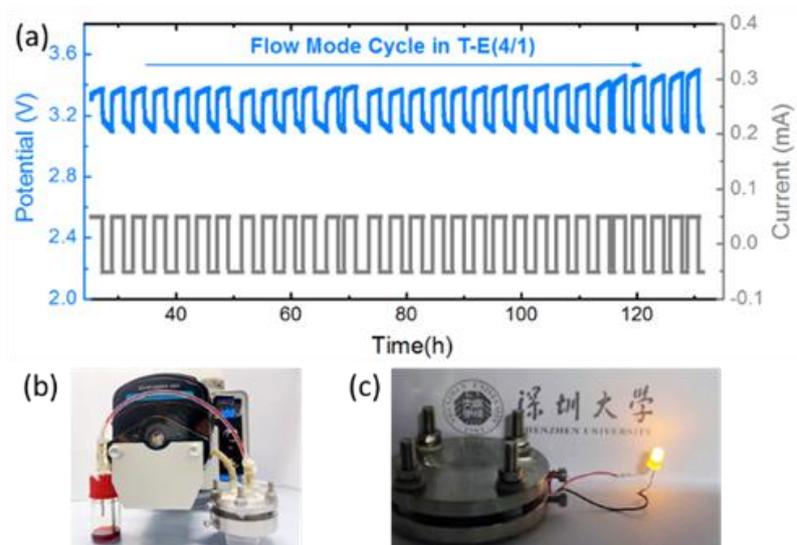
Fig. S10. (a) Flow mode test of 0.1 M Li$^+$+0.1 M TBA$^+$ in T-E (4/1) in Li-catholyte flow cell. (b) A photograph of Li-catholyte flow cell system. (c) A photograph of LED bulb powered by Li-catholyte flow cell with 0.1 M Li$^+$+0.1 M TBA$^+$ in T-E (4/1).
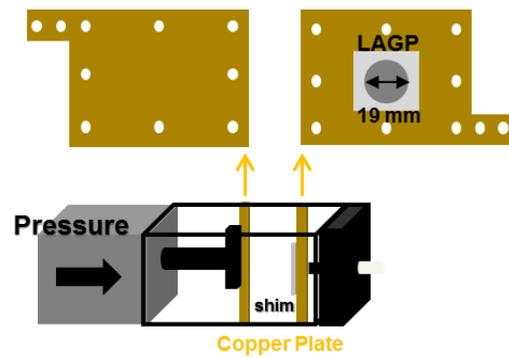
LAGP	Conductivity(S cm^{-1})
Pristine	3.59×10^{-4}
After Cycling	3.14×10^{-4}

Fig. S11. Schematic illustration of conductivity measurement process and conductivity of LAGP at pristine and after cycling stage.

15
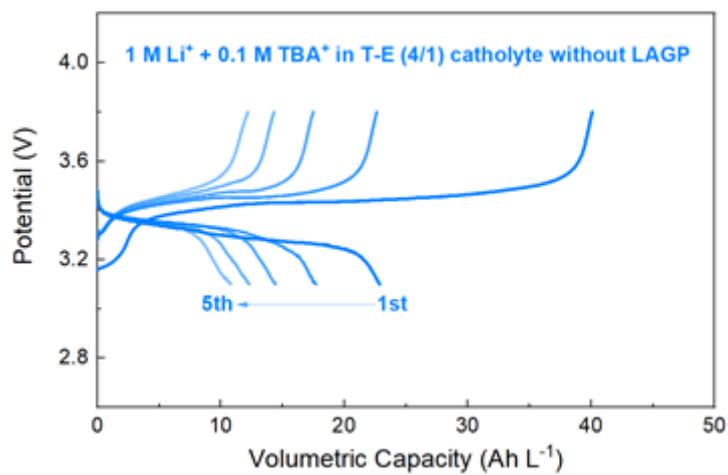
Fig. S12. Galvanostatic charge-discharge profiles of 1.0 M Li$^+$ + 0.1 M TBA$^+$ in T-E (4/1) at 0.1 mA cm^{-2} in Li-catholyte static cell without LAGP separator.
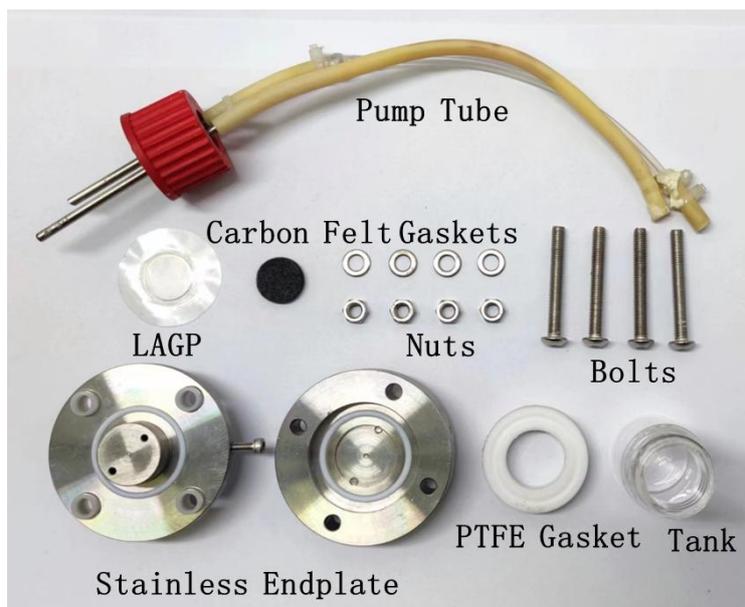
Fig. S13. A photograph of Li-catholyte flow cell.

Table S1. Estimation of the chemical cost of 2 M TEMPO in 2 M LiPF$_6$ EC/DEC, 2 M LiPF$_6$ + 0.5 M TBAPF$_6$ in T-E (4/1) and VRFB electrolytes

2 M TEMPO in 2 M LiPF$_6$ EC/DEC	Molar concentration: $c_{(tempo)}$ = 2.0 M Theoretical volumetric capacity= 53.6 Ah L^{-1}	
	Price	Chemical cost ($ Ah^{-1})
Solvent (EC)	$1.07 kg^{-1}	($1.07 kg^{-1}×1.32 kg L^{-1}+ $1.15 kg^{-1}×0.98 kg L^{-1}
Solvent (DEC)	$1.15 kg^{-1}	+$22.87 kg^{-1}×0.31kg L^{-1}+ $3.66 kg^{-1}×0.32 kg L^{-1})
Salts (LiPF$_6$)	$22.87kg^{-1}	$\times \dfrac{1}{53.6 \text{ Ah L}^{-1}}$ =$ 0.19 Ah^{-1}
Active materials (TEMPO)	$3.66 kg^{-1}	
2 M Li$^+$ + 0.5 M TBA$^+$ in T-E (4/1)	Molar concentration: $c_{(Li^+ + TBA^+)}$ = 2.5 M Theoretical volumetric capacity= 67.0 Ah L^{-1}	
	Price	Chemical cost ($ Ah^{-1})
Solvent (EC)	$1.07 kg^{-1}	($1.07 kg^{-1}×0.132 kg L^{-1}+ $1.15 kg^{-1}×0.098 kg L^{-1}+
Solvent (DEC)	$1.15 kg^{-1}	$3.66 kg^{-1}×0.32 kg L^{-1}+$57.95 kg^{-1}×0.19 kg L^{-1}
Salts (LiPF$_6$)	$22.87 kg^{-1}	+$22.87 kg^{-1}×0.77 kg L^{-1}) $\times \frac{1}{67.0 \text{ Ah L}^{-1}}$
Salts (TBAPF$_6$)	$57.95 kg^{-1}	=$ 0.45 Ah^{-1}
Active materials (TEMPO)	$3.66 kg^{-1}	
VRFB	Molar concentration: $c_{(VO^{2+})}$ = 1.0 M Theoretical volumetric capacity= 26.8 Ah L^{-1}	
	Price	Chemical cost ($ Ah^{-1})
Solvent (H$_2$O)	$0 kg^{-1}	($2.3 kg^{-1}×0.294 kg L^{-1}+$88.44 kg^{-1}×0.163 kg L^{-1})
Salts (H$_2$SO$_4$, 3 M)	$2.3 kg^{-1}	$\times \dfrac{1}{26.8 \text{ Ah L}^{-1}}$ =$0.56 Ah^{-1}
Active materials (VOSO$_4$)	$88.44 kg^{-1}	

* The calculation of the chemical cost of electrolytes was based on the price of the raw active materials (All the prices are adopted from www.alibaba.com) and the theoretical volumetric capacity of the electrolytes (Z. Li, G. Weng, Q. Zou, G. Cong and Y.C. Lu, A high-energy and low-cost polysulfide/iodide redox flow battery, *Nano Energy*, 30 (2016), 283-292.).